FACTA UNIVERSITATIS
Series: **Electronics and Energetics** Vol. 36, Nº 3, September 2023, pp. 315-328
https://doi.org/10.2298/FUEE2303315L

Invited paper

INFLUENCE OF SOIL CONDUCTIVITY IN CAPACITIVE COUPLING BETWEEN POWER LINES AND PIPELINES

Giovanni Lucca

Piacenza, Italy

Abstract. *Generally, when studying the capacitive coupling between power lines and pipelines the soil is considered a perfect conductor and its real conductivity is ignored; in this paper we want to overcome this limitation and present a study about the influence of soil conductivity just in the context of the above mentioned phenomenon. In order to do that, we derive analytical formulas for calculating the electric scalar potential, both in the air and in the ground, generated by an overhead conductor, and we compare some results obtained by means of these formulas with the ones deriving from the well known method of images that is based on the assumption of perfectly conducting soil.*

Key words: *electromagnetic interference, capacitive coupling, electromagnetic compatibility, power lines, pipelines*

1. INTRODUCTION

A typical Electromagnetic Compatibility (EMC) problem, at power frequencies (50-60Hz), is represented by the electromagnetic interference generated by power lines/electrified railway lines (sources of the interference) on pipelines and metallic telecommunication cables (victims of the interference); as a consequence of this phenomenon, dangerous over-voltages and over-currents can be generated on the victim line, thus representing a risk for staff operating along it and for equipment/apparatuses connected to the induced plant [1-2]. In the specific case of pipelines, also an incremented risk of AC corrosion due to induced voltage has to be considered [3-4].

The basic assumption common to the various models available in literature to study these problems [5-8] is the quasi-static approximation; according to it, the electromagnetic coupling between source and victim of the interference can be split into: inductive (or magnetic), conductive (also said resistive or galvanic) and capacitive (or electric) coupling and each one of them may be analyzed separately.

While inductive and conductive couplings are studied by taking into account the ground conductivity, when dealing with capacitive coupling, the ground is considered a

Received May 18, 2023; revised July 12, 2023; accepted July 28, 2023
Corresponding author: Giovanni Lucca
Piacenza, Italy
E-mail: vanni_lucca@inwind.it

perfect conductor [6], [9]. Even if such an assumption leads to correct results which are confirmed by field experience, from the logical and theoretical point of view, this is contradictory because, in the context of the same physical phenomenon (i.e. the whole electromagnetic interference sum of inductive, conductive and capacitive couplings), the ground is considered, on one side, a medium having finite conductivity and on the other side a perfect conductor.

The purpose of this paper is to propose a different approach to the modeling of the capacitive coupling which is no more based on the hypothesis of ground as a perfect conductor, but, on the contrary, the soil conductivity and permittivity are taken into account. In such a way, it is possible to have an idea of the influence of the aforementioned parameters which, on the contrary, is hidden in the approach based on the hypothesis of a perfectly conductive ground.

2. Mathematical Formulation of the Problem

As the plants that are sources of the electromagnetic field (power/railway lines) have the characteristic of being long filamentary structures, they can be represented, for our purposes, by means of the transmission line model; as known, the advantage of the transmission line model is the cylindrical symmetry so that the electromagnetic field generated by the structure is equal in any transveral plane perpendicular to the line axis. In such a way, the geometry of the problem from tridimensional can be simplified into bidimensional.

Moreover, as in this paper we are dealing solely with capacitive coupling, the only electromagnetic quantity to be considered is the scalar electric potential V; thus in the following we are going to focus on the differential equations and on their solutions relevant to V in both the media involved in the problem that is: air and ground.

Another assumption adopted is that all the materials involved are homogeneous, linear and isotropic; nevertheless, when considering the soil conductivity and relative permettivity it is necessary to mention that they are not constant but have a frequency dependent behaviour. In fact, according to a frequently used model for soil parameters proposed by Visacro and Alipio [10-11], both the above mentioned parameters can be expressed by means of simple analytical formulas (see Appendix A), in the range [100Hz, 4MHz]. Nevertheless our analysis will be restricted to frequencies lesser than 10kHz because this is the range of interest of electromagnetic interference produced by power/railway lines on pipelines.

For simplicity we shall consider a source represented by a single conductor, but the results presented in this paragraph can be immediately extended to the case of a source composed by more than one conductor by simply applying the superposition principle.

In Fig. 1, a simple representation of the geometry of the problem is shown. In the drawing we can see that the air is characterized by the electrical parameters (σ_0, μ_0, ε_0) being its conductivity σ_0=0 while μ_0 and ε_0 are the vacuum absolute magnetic permeability and permittivity respectively; as far as the ground is concerned, it is characterized by conductivity σ_1, magnetic permeability μ_1 (that will be assumed equal to μ_0) and permittivity $\varepsilon_1=\varepsilon_0\varepsilon_{r1}$ being ε_{r1} its relative dielectric constant.

Finally, the conductor axis, having coordinates (D, H), is carrying a per unit length (p.u.l.) linear current density ρ_{lin}.

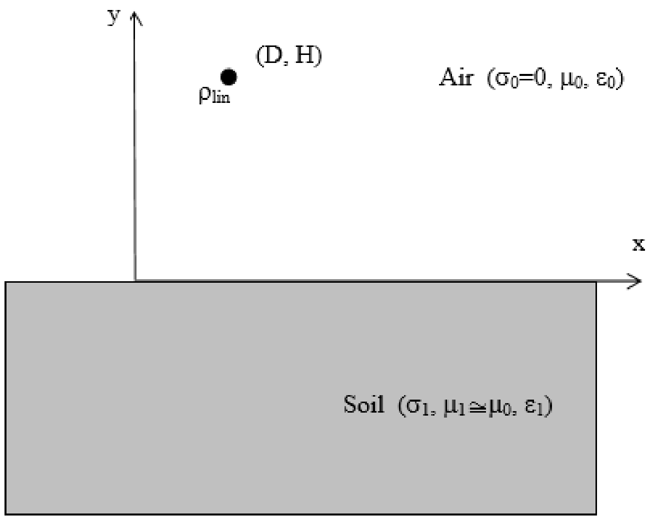

Fig. 1 Sketch of the geometry of the problem

For the following, it is necessary to introduce these parameters:

$$k_o^2 = -j\omega\mu_0(j\omega\varepsilon_0) = \omega^2\mu_0\varepsilon_0 \tag{1}$$

$$k_1^2 = -j\omega\mu_1(\sigma_1 + j\omega\varepsilon_1) \cong \omega^2\mu_0\varepsilon_0\left(\varepsilon_{r1} - \frac{j\sigma_1}{\omega\varepsilon_0}\right) \tag{2}$$

Being j the imaginary unit, $\omega=2\pi f$ the angular frequency and f the frequency.

It is also worthwhile to define the complex relative ground permittivity $\hat{\varepsilon}_{r1}$ by means of:

$$\hat{\varepsilon}_{r1} = \left(\varepsilon_{r1} - \frac{j\sigma_1}{\omega\varepsilon_0}\right) \tag{3}$$

From Maxwell equations expressed in phasor form and by assuming a time dependence of the type exp(jωt), it is possible to obtain the partial differential equations for the potential $V_i=V_i(x, y)$ in both the media: air (i=0) and ground (i=1).

For the air we have:

$$\frac{\partial^2 V_0(x,y)}{\partial x^2} + \frac{\partial^2 V_0(x,y)}{\partial y^2} + k_0^2 V_0(x,y) = -\frac{\rho_{lin}}{\varepsilon_0}\delta(x-D)\delta(y-H) \tag{4}$$

Being δ the Dirac delta.

Note that by writing equation (4), we have assumed that the p.u.l. linear charge density ρ_{lin} carried by the conductor, can be expressed by:

$$\rho_{lin}(x,y) = \rho_{lin}\delta(x-D)\delta(y-H) \tag{5}$$

For the ground we have:

$$\frac{\partial^2 V_1(x,y)}{\partial x^2}+\frac{\partial^2 V_1(x,y)}{\partial y^2}+k_1^2 V_1(x,y)=0 \tag{6}$$

To complete the formulation, we have to add the boundary conditions at the air-ground interface that is for y=0.

The first one is the continuity condition of the potential which yields:

$$V_0(x,0)=V_1(x,0) \tag{7}$$

The second one is the condition relating the continuity of the normal derivative of the scalar potential at the interface between two media having finite conductivities [12]; in our case, such a condition can be written as:

$$\varepsilon_0\frac{\partial V_0(x,0)}{\partial y}=\varepsilon_0\hat{\varepsilon}_{r1}\frac{\partial V_1(x,0)}{\partial y} \tag{8}$$

Lastly, at infinity, the potential both in air and ground must vanish so that we have:

$$\lim_{x\to\pm\infty} V_0(x,y)=0 \qquad \lim_{y\to+\infty} V_0(x,y)=0 \tag{9}$$

$$\lim_{x\to\pm\infty} V_1(x,y)=0 \qquad \lim_{y\to-\infty} V_1(x,y)=0 \tag{10}$$

3. Expressions of the Scalar Potential

3.1. Exact expressions

In this paragraph we present, in a concise way, the main steps to obtain the solutions of equations (4) and (6).

As far as equation (4) is concerned, its solution is given by the sum of a particular solution and a solution of its associated homogeneous equation.

A particular solution $V_{p0}(x, y)$ of equation (4) fullfilling the conditions expressed in equations (9) is [13]:

$$V_{p0}(x,y)=\frac{\rho_{lin}}{2\pi\varepsilon_0}K_0\left(j\omega\sqrt{\mu_0\varepsilon_0}\sqrt{(x-D)^2+(y-H)^2}\right) \tag{11}$$

where K_0 is the modified Bessel function of second kind and 0 order (see Appendix B).

For the following, it is useful to write also an integral representation of $V_{0p}(x,y)$ [14] that is:

$$V_{0p}(x,y)=\frac{\rho_{lin}}{2\pi\varepsilon_0}\int_0^\infty \frac{e^{-|y-H|\sqrt{\lambda^2-k_0^2}}}{\sqrt{\lambda^2-k_0^2}}\cos\left[\lambda(x-D)\right]d\lambda \tag{12}$$

Regarding the solution $V_{0h}(x, y)$ of the associated homogeneous equation, by using the separation variable technique and by taking into account the conditions given by equations (9), one has:

$$V_{0h}(x,y) = 2\int_0^\infty E(\lambda) e^{-\sqrt{\lambda^2 - k_0^2}\,(y-H)} \cos\left[\lambda(x-D)\right] d\lambda \tag{13}$$

being $E(\lambda)$ a function to be determined from boundary conditions at air-ground interface.

In a similar way, the solution of equation (6), that fullfills the conditions expressed by formulas (10), is:

$$V_1(x,y) = 2\int_0^\infty F(\lambda) e^{\sqrt{\lambda^2 - k_1^2}\,(y-H)} \cos\left[\lambda(x-D)\right] d\lambda \tag{14}$$

being $F(\lambda)$ a second function to be determined from boundary conditions at air-ground interface.

The functions $E(\lambda)$ and $F(\lambda)$ are solutions of the following linear system obtained by taking into account of equations (12), (13) and (14) and by imposing the boundary conditions represented by equations (7) and (8):

$$\begin{cases} 2E(\lambda) e^{\sqrt{\lambda^2 - k_0^2}H} - 2F(\lambda) e^{-\sqrt{\lambda^2 - k_1^2}H} = -\dfrac{\rho_{lin}}{2\pi\varepsilon_0} e^{-\sqrt{\lambda^2 - k_0^2}H} \dfrac{1}{\sqrt{\lambda^2 - k_0^2}} \\ 2\varepsilon_0 \sqrt{\lambda^2 - k_0^2}\, E(\lambda) e^{\sqrt{\lambda^2 - k_0^2}H} + 2\varepsilon_0 \hat{\varepsilon}_{r1} \sqrt{\lambda^2 - k_1^2}\, F(\lambda) e^{-\sqrt{\lambda^2 - k_1^2}H} = \dfrac{\rho_{lin}}{2\pi} e^{-\sqrt{\lambda^2 - k_0^2}H} \end{cases} \tag{15}$$

By solving this system one gets:

$$\begin{cases} E(\lambda) = \dfrac{\rho_{lin}}{4\pi\varepsilon_0} \dfrac{\sqrt{\lambda^2 - k_0^2} - \hat{\varepsilon}_{r1}\sqrt{\lambda^2 - k_1^2}}{\sqrt{\lambda^2 - k_0^2} + \hat{\varepsilon}_{r1}\sqrt{\lambda^2 - k_1^2}} \dfrac{e^{-2H\sqrt{\lambda^2 - k_0^2}}}{\sqrt{\lambda^2 - k_0^2}} \\ F(\lambda) = \dfrac{\rho_{lin}}{2\pi\varepsilon_0} \dfrac{e^{H()\left(\sqrt{\lambda^2 - k_1^2} - \sqrt{\lambda^2 - k_0^2}\right)}}{\hat{\varepsilon}_{r1}\sqrt{\lambda^2 - k_1^2} + \sqrt{\lambda^2 - k_0^2}} \end{cases} \tag{16}$$

By adding equations (12) and (13) and by taking into account of the first relationship expressing $E(\lambda)$ in formula (16), one can write the expression for the potential in the air $V_0(x, y)$:

$$\begin{aligned} V_o(x,y) = {} & \frac{\rho_{lin}}{2\pi\varepsilon_0} K_0\left(j\omega\sqrt{\mu_0\varepsilon_0}\sqrt{(x-D)^2 + (y-H)^2} \right) + \\ & \frac{-\rho_{lin}}{2\pi\varepsilon_0} K_0\left(j\omega\sqrt{\mu_0\varepsilon_0}\sqrt{(x-D)^2 + (y+H)^2} \right) + \\ & + \frac{\rho_{lin}}{2\pi\varepsilon_0} \int_0^\infty \frac{2e^{-\sqrt{\lambda^2 - k_0^2}\,(y+H)}}{\sqrt{\lambda^2 - k_0^2} + \hat{\varepsilon}_{r1}\sqrt{\lambda^2 - k_1^2}} \cos\left[\lambda(x-D)\right] d\lambda \end{aligned} \tag{17}$$

Notice that the first addend in equation (17) represents the primary contribution of a source having p.u.l. charge density ρ_{lin} placed at coordinates (D, H) in an infinite space, having the characteristics of the air, while the second addend represents, in the same space, an image source placed at coordinates (D, -H) and carrying an opposite p.u.l. charge density $-\rho_{lin}$. The role played by the second addend is to simulate the presence of the ground modelled as a perfect conductor; notice that both the terms do not depend on the soil conductivity σ_1.

On the contrary the third addend in equation (17) depends on σ_1 and it can be considered a further correction term related to the presence of the ground.

Coming to the potential in the ground $V_1(x, y)$, by substituting the expression for $F(\lambda)$ contained in formula (16), one obtains:

$$V_1(x,y) = \frac{\rho_{lin}}{2\pi\varepsilon_0}\int_0^\infty \frac{2e^{-\sqrt{\lambda^2-k_0^2}H} e^{\sqrt{\lambda^2-k_1^2}y}}{\sqrt{\lambda^2-k_0^2}+\hat{\varepsilon}_{r1}\sqrt{\lambda^2-k_1^2}}\cos\left[\lambda(x-D)\right]d\lambda \tag{18}$$

3.2. Closed form approximated expressions

It possible to give some closed form approximated expressions for both $V_0(x, y)$ and $V_1(x, y)$; the usefulness of such approximated expressions is related to the difficulty in calculating the scalar potential by means of the exact formulas given by expressions (17) and (18); the problematic in calculating the two integrals contained in them (Sommerfeld integrals) consists in the fact they slowly converge and the integrands have a strongly oscillating behaviour; thus, they may require a certain computational effort especially if they have to be evaluated inside the same program many times in correspondence of different points and/or different frequencies. For such a reason it is worthwile to have at disposal also easier expressions that may be used in practical applications.

As far as $V_0(x, y)$ is concerned and by considering the third addend, we have that in most of the integration range for λ the following approximation holds:

$$\sqrt{\lambda^2-k_0^2} \cong \sqrt{\lambda^2-k_1^2} \tag{19}$$

Thus, we may write:

$$\int_0^\infty \frac{2e^{-\sqrt{\lambda^2-k_0^2}(y+H)}}{\sqrt{\lambda^2-k_0^2}+\hat{\varepsilon}_{r1}\sqrt{\lambda^2-k_1^2}}\cos\left[\lambda*(x-D)\right]d\lambda \cong \frac{2K_0\left(j\omega\sqrt{\mu_0\varepsilon_0}\sqrt{(x-D)^2+(y-H)^2}\right)}{\sqrt{\lambda^2-k_0^2}+\hat{\varepsilon}_{r1}\sqrt{\lambda^2-k_1^2}} \tag{20}$$

and consequently, by substituting (20) in place of the third term in formula (17), we obtain the following approximate expression for $V_0(x, y)$:

$$\begin{aligned} V_{0app}(x,y) &\cong \frac{\rho_{lin}}{2\pi\varepsilon_0}K_0\left(j\omega\sqrt{\mu_0\varepsilon_0}\sqrt{(x-D)^2+(y-H)^2}\right)+ \\ &-\frac{\hat{\varepsilon}_{r1}-1}{\hat{\varepsilon}_{r1}+1}\frac{\rho_{lin}}{2\pi\varepsilon_0}K_0\left(j\omega\sqrt{\mu_0\varepsilon_0}\sqrt{(x-D)^2+(y+H)^2}\right) \end{aligned} \tag{21}$$

The first term in equation (21) represents the primary contribution of the source, while the second term represents the contribution of a image source placed in specular position with respect to the air-ground interface; the intensity of the image source ρ_{lin} is reduced of a factor R given by:

$$R = \frac{\hat{\varepsilon}_{r1} - 1}{\hat{\varepsilon}_{r1} + 1} \tag{22}$$

Notice that the factor R still depends on ω, σ_1 and ε_{r1} (see equation 3).

It is possible to further simplify the relationship given by equation (21) obtaining the expression that could be directly derived by applying the well known *method of images* [15]. In fact, for low frequencies and in the ordinary range of values for σ_1 and ε_{r1} we have that:

$$\left| j\omega\sqrt{\mu_0\varepsilon_0}\sqrt{(x-D)^2 + (y \pm H)^2} \right| << 1 \qquad R \cong 1 \tag{23}$$

Therefore, by substituting in formula (21) the modified Bessel functions K_0 with its small argument approximation [16] (see also Appendix B formula (B4)) and by using the second relationship in formula (23), we obtain the following expression $V_{0mi}(x,y)$ for the potential in air:

$$V_{0mi} = \frac{\rho_{lin}}{2\pi\varepsilon_0} \ln\left(\sqrt{\frac{(x-D)^2 + (y+H)^2}{(x-D)^2 + (y-H)^2}} \right) \tag{24}$$

Notice that this expression does not depend on frequency f, on ground conductivity σ_1 and on ground permittivity ε_1.

As far as $V_1(x, y)$ is concerned, starting from equation (18) we have that in most of the integration range for λ, the approximation expressed by formula (19) holds; thus, we obtain the following equation for $V_{1app}(x, y)$:

$$\begin{aligned} V_{1app}(x,y) &= \frac{\rho_{lin}}{2\pi\varepsilon_0} \int_0^\infty \frac{2e^{\sqrt{\lambda^2 - k_1^2}(y-H)}}{(1+\hat{\varepsilon}_{r1})\sqrt{\lambda^2 - k_1^2}} \cos\left[\lambda(x-D)\right] d\lambda = \\ &= \frac{\rho_{lin}}{2\pi\varepsilon_0} \frac{2}{\hat{\varepsilon}_{r1}+1} K_0\left(j\omega\sqrt{\mu_0\varepsilon_0\hat{\varepsilon}_{r1}}\sqrt{(x-D)^2 + (y-H)^2} \right) \end{aligned} \tag{25}$$

Notice that this expression still depends on frequency f, on ground conductivity σ_1 and on ground permittivity ε_1.

4. Comparison among Different Expressions

In this section we present some comparisons among the different expressions for the scalar potential previously presented.

The integrals appearing in formulas (17) and (18) have been numerically evaluated by means of the trapezoidal rule by using an extremely small integration step equal to 10^{-5} covering the integration range [0, 8]; we have verified that the contribution to the integral outside that integration range was negligible.

As mentioned before, the comparison is oriented to very low frequencies and covers the range [10Hz, 10kHz]; in this interval we did not find problems of numerical instability concerning the integrals in formulas (17) and (18).

Firstly, let us define the per cent relative difference between the exact formula and the corresponding approximate one; thus we have for the air two cases:

$$\Delta\%_{0app}(x,y) = 100\left(\frac{|V_0(x,y)| - |V_{0app}(x,y)|}{|V_0(x,y)|}\right) \tag{26}$$

$$\Delta\%_{0mi}(x,y) = 100\left(\frac{|V_0(x,y)| - |V_{0mi}(x,y)|}{|V_0(x,y)|}\right) \tag{27}$$

while, for the ground, we have:

$$\Delta\%_{1app}(x,y) = 100\left(\frac{|V_1(x,y)| - |V_{1app}(x,y)|}{|V_1(x,y)|}\right) \tag{28}$$

We have considered a source placed at D=0m and H=20m and soil parameters having frequency dependence according to the formula of Visacro-Alipio (see Appendix A) and characterized by different values of $\sigma_{100\text{Hz}}$ ($\sigma_{100\text{Hz}}$ is the value of soil conductivity for f=100Hz) i.e.: 10^{-4}S/m, 10^{-3}S/m, 10^{-2}S/m and with relative dielectric constant ε_{r1}=192[1]. Moreover, in the examples that follow, we have reasonably assumed that in the range [0Hz, 100Hz] the value of the soil conductivity is constant and equal to $\sigma_{100\text{Hz}}$.

In Fig. 2 the values of $\Delta\%_{0\,\text{app}}$ and $\Delta\%_{0\,\text{mi}}$ have been plotted versus lateral distance from the source for different values of $\sigma_{100\text{Hz}}$ and for f=50Hz.

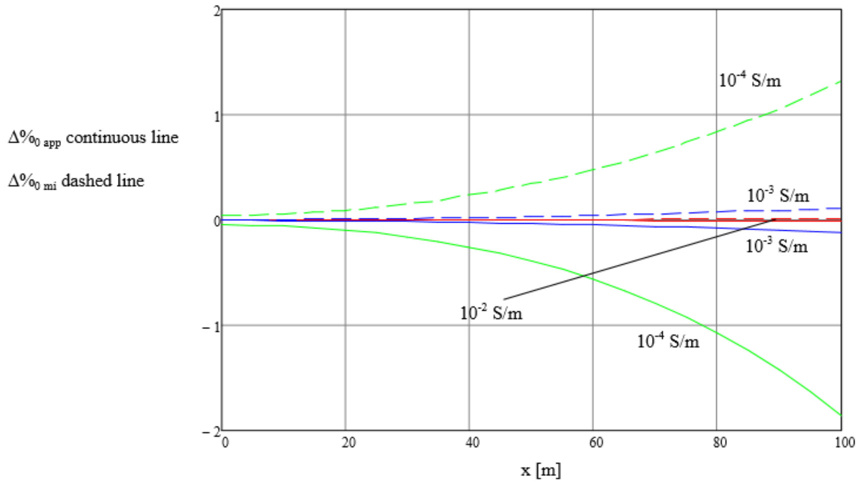

Fig. 2 Percent relative difference versus lateral distance for different values of $\sigma_{100\text{Hz}}$; f=50Hz, y=1m

Fig. 2 shows that at 50Hz both the approximations are very good; the quantities $\Delta\%_{0\,app}$ and $\Delta\%_{0\,mi}$ show an increasing trend by increasing the distance from the source and by decreasing the value of $\sigma_{100\text{Hz}}$.

---

[1] This is the suggested value coming from the Visacro-Alipio formula for frequencies lower than 10kHz

In Fig. 3 the values of $\Delta\%_{0\ app}$ and $\Delta\%_{0\ mi}$ have been plotted versus the frequency, for different values of soil conductivity and for x=50m, y=1m.

By looking at Fig. 3, we can see that for soils having medium-high values of σ_{100Hz} both the approximations are very good till to some kHz, while for soils of very low values of σ_{100Hz} both the approximations are very good till to some hundreds of Hz.

In Fig. 4 the values of $\Delta\%_{1\ app}$ have been plotted versus lateral distance from the source for different values of σ_{100Hz} and for f=50Hz.

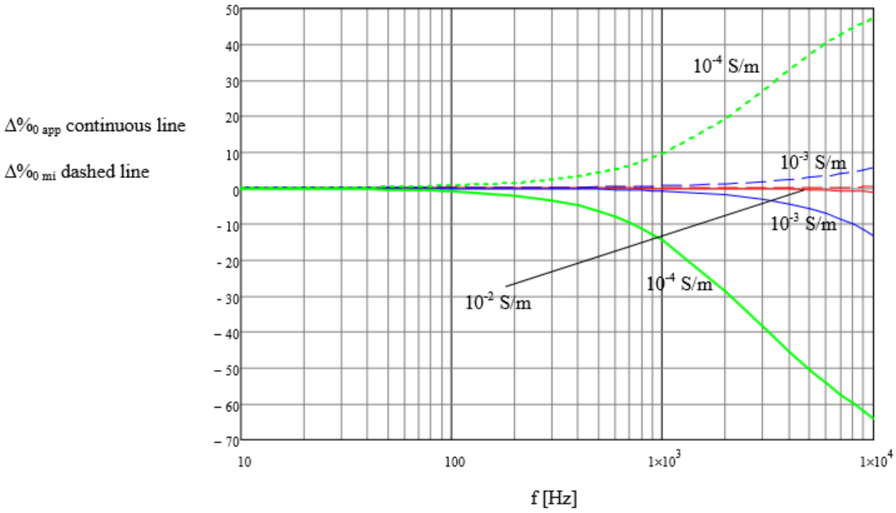

Fig. 3 Percent relative difference versus frequency for different values of σ_{100Hz}; x=50m, y=1m

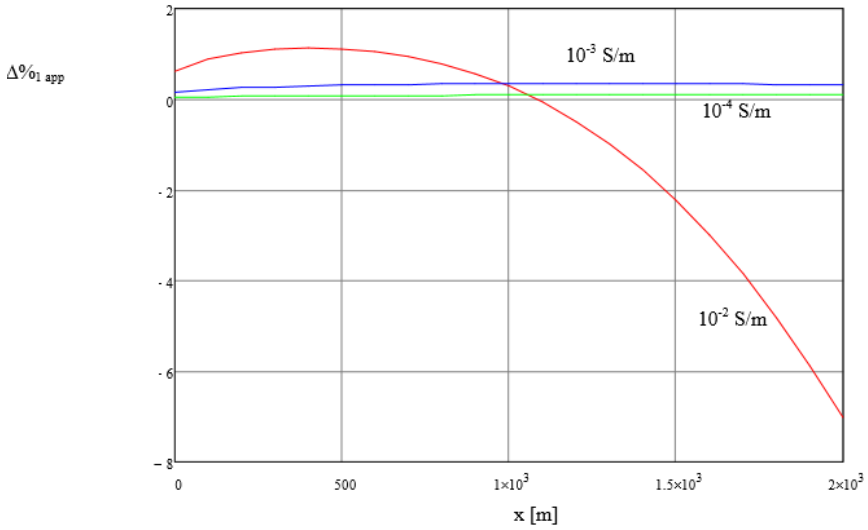

Fig. 4 Percent relative difference versus lateral distance for different values of σ_{100Hz}; f=50Hz, y=-1m

Fig. 4 shows that at 50 Hz the approximation is very good especially for medium-low values of σ_{100Hz}; the differences tend to increase by increasing the distance from the source; such a trend is much more evident for high values of σ_{100Hz}.

In Fig. 5 the values of $\Delta\%_{1\ app}$ have been plotted versus the frequency, for different values of σ_{100Hz} and for x=10m, y=-1m.

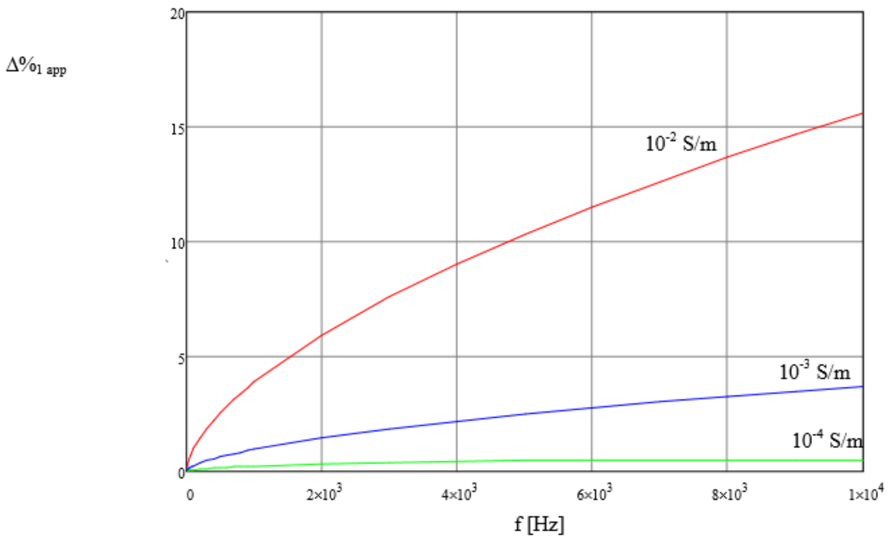

Fig. 5 Percent relative difference versus frequency for different values of soil σ_{100Hz}; x=10m, y=-1m.

By looking at Fig. 5, we can see that for soils having high values of σ_{100Hz} the approximation is good till to about 1 kHz, while for soils having medium-low values of σ_{100Hz} the approximations are very good till to 10 kHz.

5. Capacitive Coupling between Power Line and Pipeline

5.1. Basic assumptions and formulas

In this paragraph we present two examples of calculation of capacitive interference generated by an High Voltage (HV) power line on a pipeline; in order to have only capacitive coupling, we consider the ideal case where the HV line axis is exactly perpendicular to the pipeline (see Fig. 6) so that no inductive interference exists; moreover, we suppose that the HV line is under normal operating condition so that no currents, injected into soil through the tower grounding electrodes as in case of fault of a phase to ground, are present and consequently neither conductive coupling exists.

In both the examples that follow, the inducing source is represented by a tri-phase 380kV-50Hz line provided with two shield wires while the pipeline, having length L, shall be considered overhead (height h>0) in the first example and buried in the soil (burial depth h<0) in the second example.

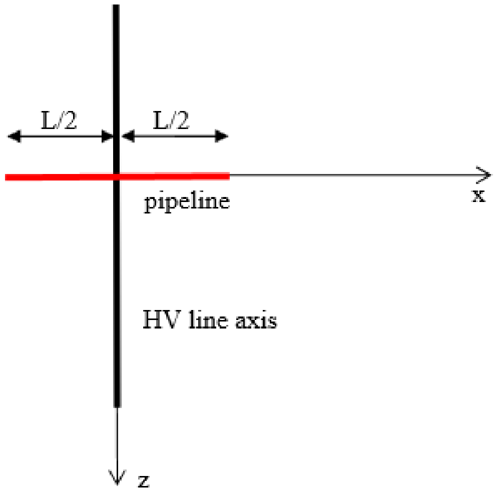

Fig. 6 Sketch of HV line and pipeline layouts

The pipeline has no grounding points and the voltage induced along it *U*=*U*(*x*) can be calculated by means of the following formula (see [5]) that represents the analytical solution of a two-wire transmission line of length *L*, open circuited at both the terminations and drived by a distributed ideal current generator *J*(x) (see next formula (33)).

$$U(x) = G_1(x) + \frac{G_2(L)}{\sinh(\gamma L)}\cosh(\gamma x) \tag{29}$$

where γ is the propagation constant of the pipeline circuit with ground return given by:

$$\gamma = \sqrt{Z\,Y} \tag{30}$$

being *Z* and *Y* respectively the p.u.l. impedance and admittance of the circuit itself.

The quantities $G_1(x)$ and $G_2(x)$ are given by [5]:

$$G_1(x) = \frac{e^{-\gamma x}}{2}\int_0^x \sqrt{\frac{Z}{Y}}J(\alpha)e^{\gamma a}d\alpha + \frac{e^{\gamma x}}{2}\int_0^x -\sqrt{\frac{Z}{Y}}J(\alpha)e^{-\gamma a}d\alpha \tag{31}$$

$$G_2(x) = \frac{e^{-\gamma x}}{2}\int_0^x \sqrt{\frac{Z}{Y}}J(\alpha)e^{\gamma a}d\alpha - \frac{e^{\gamma x}}{2}\int_0^x -\sqrt{\frac{Z}{Y}}J(\alpha)e^{-\gamma a}d\alpha \tag{32}$$

and

$$J(x) = YV(x,h) \tag{33}$$

is the p.u.l. current generator applied to the pipeline-ground circuit that models the capacitive influence generated by the HV line. In fact, in equation (33) *V*=*V*(*x*, *h*) is the potential generated at the location of the pipeline axis by the power line that can be calculated according to the formulas presented in the previous section 3.

5.2. Overhead pipeline

The case of an overhead pipeline in proximity of a HV powerline and with no connections to ground is often encounted before the burial operations of the pipe. For example a relatively short conductor, such as a single joint of line pipe supported by a nonmetallic sling or on a rubber- tired vehicle.

Thus, we consider a single joint of pipe having length L=20m and placed at height 1.5m above ground. By calculating the potential in the air produced by the HV line according to the formulas presented in par. 3 and applying formula (29) we obtain a voltage practically constant along the whole length of the pipe. In Table 1, the induced pipe voltage is shown for different values of σ_{100Hz} that, as already mentioned, we have assumed to be valid also for f=50Hz so that $\sigma_1=\sigma_{100Hz}$.

Table 1 Induced voltage for different value of soil conductivity; overhead pipeline

σ_1 [S/m]	Voltage [V]
10^{-2}	124.93
10^{-3}	124.95
10^{-4}	125.21
10^{-5}	129.01

If one applies the method of images to calculate the potential in air, the result for the induced voltage along the pipe is a constant value equal to 124.95V that does not depend on σ_1.

In contrast to the method of images, the results in Table 1 show a very weak but non-zero dependence on the soil conductivity and the values of induced voltage increase by decreasing the soil conductivity.

5.3. Buried pipeline

We consider a buried pipeline section 4km long between two insulating joints; in such a way one can study this portion of pipe ignoring the remaining part of the the route.

Also in this case, calculations show that the induced voltage along the pipe is practically constant and the results for different values of soil conductivity are shown in Table 2.

Table 2 Induced voltage for different value of soil conductivity; buried pipeline

Soil conductivity σ_1 [S/m]	Voltage [V]
10^{-2}	0.0007
10^{-3}	0.021
10^{-4}	0.393
10^{-5}	5.91

By looking at Table 2 we can notice the very small values for the induced voltage; that explains why in practical applications the capacitive coupling between power lines and buried pipelines is usually ignored. Anyway, we can notice that the influence of the soil actually exists with an increasing trend that follows the decrease of the conductivity.

6. CONCLUSIONS

In this paper, we have presented a study about capacitive coupling, at power frequencies, between power lines and pipelines, that differently from what commonly appears in literature, does not model the ground as perfect conductor but it takes into account its conductivity and permittivity.

The results obtained by comparing the model of perfectly conducting ground and the model of soil with non-zero conductivity show that the differences are very small at power frequencies. Nevertheless, in applications where higher frequencies are involved (higher harmonics, transients), the model here presented seems more adequate because in these cases the influence of the ground conductivity and permittivity is not so negligible.

APPENDIX A

According to the work of Visacro-Alipio [10-11] about the frequency dependence of soil parameters relevant to lightning response of grounding electrodes, one has that ground conductivity and relative permettivity are not constant quantities but depend on the frequency. On the basis of many measurements and subsequent analysis, the authors found an empirical formula able to describe their frequency dependence in the range [100Hz-4MHz].

By using the resistivity ρ, instead of the conductivity σ, they proposed the following expressions:

$$\rho(f) = \rho_{100Hz}\left\{1 + [1.2 \cdot 10^{-6} \cdot \rho_{100Hz}^{0.73}](f - 100)^{0.65}\right\}^{-1} \quad \text{(A1)}$$

$$\varepsilon_{r1}(f) = \begin{cases} 7.6 \cdot 10^{3} \cdot f^{-0.4} + 1.3 & f > 10kHz \\ 192.203 & f \le 10kHz \end{cases} \quad \text{(A2)}$$

In formula (A1) the quantity ρ_{100Hz} is the value of soil resistivity for f=100Hz; in the rest of our paper, we used, for convenience, its reciprocal σ_{100Hz}.

APPENDIX B

We report here from [17] the explicit formula for K_0 that is the modified Bessel function of second kind and zero order.

If z is a complex number with $|\arg(z)| < \pi/2$, $K_0(z)$ is given by the following ascending series:

$$K_0(z) = -\left\{\ln\left(\frac{1}{2}z\right) + \gamma\right\} I_0(z) + \frac{\frac{1}{4}z^2}{(1!)^2} + \left(1 + \frac{1}{2}\right)\frac{\left(\frac{1}{4}z^2\right)^2}{(2!)^2} + \\ + \left(1 + \frac{1}{2} + \frac{1}{3}\right)\frac{\left(\frac{1}{4}z^2\right)^3}{(3!)^3} + \dots \quad \text{(B1)}$$

where γ=0.57721.. is the Euler-Mascheroni constant and $I_0(z)$ is the modified Bessel function of first kind and zero order that is expressed by:

$$I_0(z)=\sum_{k=0}^{\infty}\frac{\left(\frac{1}{4}z^2\right)^k}{k!\Gamma(k+1)} \tag{B2}$$

In formula (B2), Γ is the Gamma function which, for integer values of the argument, becomes the factorial function that is:

$$\Gamma(k+1)=k! \quad k=0,1,2,\ldots \tag{B3}$$

For small values of the argument *z*, formula (B1) simplifies into:

$$K_0(z)=-\left\{\ln\left(\frac{1}{2}z\right)+\gamma\right\} \tag{B4}$$

REFERENCES

[1] EN 50443, Effects of electromagnetic interference on pipelines caused by high voltage a.c. electric traction systems and/or high voltage a.c. power supply systems, CENELEC, 2012.

[2] ITU-T, Recommendation K.68, Operator responsibilities in the management of electromagnetic interference by power systems on telecommunication systems, 2008.

[3] CEN EN 15280, Evaluation of a.c. Corrosion Likelihood of Buried Pipelines Applicable to Cathodically Protected Pipelines, 2013.

[4] CIGRE, AC Corrosion on Metallic Pipelines Due to Interference from AC Power Lines—Phenomenon, Modelling and Countermeasures; Cigre Working Group C4. 2.02, Paris, France, 2006.

[5] ITU-T, Directives concerning the protection of telecommunication lines against harmful effects from electric power and electrified railway lines, Capacitive, inductive and conductive coupling: physical theory and calculation methods, vol. III, ITU, 1989.

[6] CIGRE, Guide on the influence of high voltage A. C. power systems on metallic pipeline, CIGRE, 1995.

[7] EPRI, Power Line Fault Current Coupling to Nearby Natural Gas Pipelines, Analytic Methods and Graphical Techniques vol. 1, EPRI 1987.

[8] D. Șteț, D. D. Micu, L. Czumbil, L. Darabant and A. Ceclan, "Simulation of interference between power lines and gas pipelines in unbalanced phase currents state", *COMPEL: Int. J. Comput. Math. Electr. Electron. Eng.*, vol. 31, но.4, pp. 1178-1189, 2012.

[9] D. Șteț, L. Czumbil and D. D. Micu, Evaluation of Electromagnetic Interferences Affecting Metallic Pipelines in Pipeline Engineering-Design, Failure, and Management, IntechOpen, 2022.

[10] S. Visacro and R. Alipio, "Frequency Dependence of Soil Parameters: Experimental Results, Predicting Formula and Influence on the Lightning Response of Grounding Electrodes ", *IEEE Trans. Power Del.*, vol. 27, pp. 927-935, April 2012.

[11] R. Alipio and S. Visacro "Frequency Dependence of Soil Parameters: Effect on the Lightning Response of Grounding Electrodes ", *IEEE Trans. Electromagn. Compat.*, vol. 55, pp. 132-139, Feb. 2012.

[12] C. T. A. Johnk, *Engineering Electromagnetic Fields and Waves*. John Wiley & Sons, 1975, Chapter 4, pp. 242-244.

[13] A. N. Tichonov and A. A. Samarskij, *Equazioni della fisica matematica*. Edizioni MIR, 1981, Chapter 7, pp. 507-508.

[14] I. S. Gradshteyn and I. M. Ryzhik, *Table of Integrals, Series and Products*. Academic Press, 2007, p. 491.

[15] J. D. Kraus, *Electromagnetics.* Mc Graw-Hill, 1953, Chapter 2, pp 79-80.

[16] J. Spanier and K. B. Oldham, *An atlas of functions*. Hemisphere Publishing Corporation, 1987, Chapter 51, p. 505.

[17] M. Abramowitz and I. A. Stegun, *Handbook of Mathematical Functions with Formulas, Graphs, and Mathematical Tables*. New York: Dover Publications Inc, 1972, Chapter 9, p. 375.